Synergistic in-vitro effects of combining an antiglycolytic, 3-bromopyruvate, and a bromodomain-4 inhibitor on U937 myeloid leukemia cells

Nicolette Kapp[a], Xiao X. Stander[b] and Barend A. Stander[a]

This project investigated the in-vitro effects of a glycolytic inhibitor, 3-bromopyruvate (3-BrP), in combination with and a new in silico-designed inhibitor of the bromodomain-4 (BRD-4) protein, ITH-47, on the U937 acute myeloid leukemia cell line. 3-BrP is an agent that targets the altered metabolism of cancer cells by interfering with glucose metabolism in the glycolytic pathway. ITH-47 is an acetyl-lysine inhibitor that displaces bromdomain 4 proteins from chromatin by competitively binding to the acetyl-lysine recognition pocket of this bromodomain and extraterminal (BET) BRD protein, thereby preventing transcription of cancer-associated genes and further cell growth. Cell growth studies determined the IC_{50} after 48 h exposure for 3-BrP and ITH-47 to be 6 and 2 μmol/l, respectively. When combined, 2.4 and 1 μmol/l of 3-BrP and ITH-47, respectively, inhibited 50% of the cell population, yielding a synergistic combination index of 0.9. Subsequent mechanistic studies showed that the IC_{50} concentrations of ITH-47 and 3-BrP and the combination increased observable apoptotic bodies and cell shrinkage in U937 cells treated for 48 h. Cell cycle analysis showed an increase in the sub-G_1 fraction in all treated cells, suggesting that cell death was increased in the treated samples. Annexin-V-FITC apoptosis analysis showed a statistically significant increase in the number of cells in early and late apoptosis, indicating that cell death occurred through apoptosis and not necrosis. Only U937 cells exposed to ITH-47 showed a decrease in mitochondrial membrane potential compared with the vehicle control. Reactive oxygen species production was decreased in all treated samples. ITH-47-exposed cells showed a decrease in *c-Myc*, *Bcl-2*, and *p53* gene expressions. 3-BrP-treated cells showed an increase in *c-myc* and *p53* gene expressions. The combination of ITH-47 and 3-BrP lead to downregulation of *c-myc* and *Bcl-2* genes. ITH-47 exposure conditions yielded a marked decrease in c-myc protein levels as well as a decrease in Ser70 phosphorylated Bcl-2. Analysis of 3-BrP and the combination of ITH-47 and 3-BrP test conditions indicated an increase in p53 protein levels. This novel study is the first to investigate the in-vitro synergistic therapeutic effect of ITH-47 and 3-BrP. The current study contributes toward unraveling the in-vitro molecular mechanisms and signal transduction associated with a novel combination of BRD inhibitors and antiglycolytic agents, providing a basis for further research on these combinations.

Anti-Cancer Drugs 2018, **00**:000–000

Keywords: 3-bromopyruvate, antiglycolytic, bromodomain-4 inhibitor, myeloid leukemia cells, synergism

Departments of [a]Physiology and [b]Surgery, Faculty of Health Sciences, University of Pretoria, Pretoria, South Africa

Correspondence to Andre Stander, PhD, Department of Physiology, University of Pretoria, Private Bag X323, Arcadia 0007, Pretoria, South Africa
e-mail: andre.stander@up.ac.za

Introduction

According to the World Cancer report, it was expected that more than 20 million new cases of cancer would have occurred in 2015 [1]. In first-world countries, cancer has been shown to be the number one cause of deaths annually and identified as the second major contributor to deaths in developing countries [1]. The increase in cancer-related deaths in developed countries can be traced back to the fact that the growing and aging population has adopted a higher cancer risk lifestyle; this includes smoking, lack of physical exercise, and unhealthy diets [1]. The International Agency for Research indicated that in 2030, ~21.7 million new cancer cases will be reported and the increase in cancer-related deaths will be 13 million [2]. The National Cancer Registry reported in 2011 that 437 leukemia cases were diagnosed in South African men and a total of 313 leukemia cases in South African women [3]. Millions of dollars are raised each year in the fight for cancer. the American Cancer Society reported that as of 1 August 2016, a total of $406 837 559 has been collected for cancer research, of which $25 415 735 has been allocated to research for leukemia [4]. The large funds set up for the research call for finding new and improved ways of combatting cancer, with leukemia being a research priority.

In 1827, a French physician Alfred-Armand-Louis-Marie Velpeau was the first individual to accurately describe

Supplemental Digital Content is available for this article. Direct URL citations appear in the printed text and are provided in the HTML and PDF versions of this article on the journal's website, *www.anti-cancerdrugs.com*.

acute myeloid leukemia (AML) [5]. AML is a cancer affecting the hematopoietic myeloid progenitor cells (myeloblasts). Studies have found that AML associated with exposure to benzene or chemotherapy is linked to structural changes in chromosomes five and seven [6]. Translocations cause the interruptions of genes as a section of one chromosome is transferred and exchanged with another chromosome [7]. Cigarette smoking is a source of benzene, which, studies suggest, is linked to trisomy of chromosome eight as well as a balanced translocation between chromosome 8 and chromosome 21 [8]. Cytogenic aberrations often lead to the amplification of proto-oncogenes of AML. The *Myc* genes are proto-oncogenes, which, in healthy cells, guide vital aspects of cell growth and cell cycle progression [9]. The myc protein is a transcription factor that directly binds DNA at the enhancer box sequences and activates protein transcription [10]. The c-myc protein has the ability to recruit histone acetyltransferase to add acetyl marks to lysine residues on chromatin to modify the expression of other genes [10]. A mutated version of the *Myc* gene is found in many cancers, which causes *Myc* to be constitutively expressed, leading to gene expression amplification [11]. This leads to the unregulated expression of genes involved in cell proliferation, and can result in genomic instability, causing the formation of cancer [12,13]. c-Myc is often found to be amplified and activated in AML, which in turn plays an important role in the development of leukemia [14].

The c-myc protein is a known metabolic regulator by upregulating genes encoding glucose transporters and hexokinase to increase glucose import [15], thereby contributing toward the increased glycolytic phenotype of many leukemic cancers. The Warburg effect refers to the process whereby cancer cells produce energy mostly by glycolysis and then lactic acid fermentation in the cytosol of the cell even if abundant oxygen is available [16,17]. The Warburg is well documented in solid cancers, but increased glycolytic activity has been identified in AML as well [18]. Interestingly, increased expression of the hexokinase-1 (HK1) is found in a variety of AML cell lines, including U937 cells [19]. Knockdown of this gene in U937 cells results in increased sensitivity to arabinofuranosyl cytidine [19]. Hexokinase-1 is the isoenzyme found in normal differentiated cells, whereas solid cancerous cells tend to express hexokinase-2 (HK2) predominantly [20]. HK2 is also overexpressed at a protein level in a variety of myeloid leukemia cells, whereas normal peripheral blood mononuclear cells do not express HK2 [21].

The aim of this research was to determine whether inhibiting glycolysis and abrogating c-myc expression using two different compounds can have a synergistic effect in AML (U937) cells. The first compound, ITH-47, is a newly designed BRD-4 inhibitor that can target c-myc-sensitive leukemic cancers. BRD-4 binds to acetylated histones by its bromodomain (BRD) and mediates chromatin-dependent signaling and transcription at *Myc* target loci [22]. ITH-47, a JQ1 analog, is an acetyl-lysine inhibitor, displacing the BRD and BET protein BRD-4 from chromatin, thereby indirectly preventing gene transcription of *c-myc*. The second compound, 3-bromopyruvate (BrP), is a glycolytic inhibitor targeting at least two enzymes important in glycolysis. 3-BrP inhibits HK2 by covalent modification on the cysteine residue, preventing further glucose metabolism in the glycolytic pathway [23,24]. 3-BrP also negatively affects the function of glyceraldehyde-3-phosphate dehydrogenase, decreasing the metabolic rate of glycolysis, as 3-phosphate dehydrogenase is essential for the conversion of glyceraldehyde-3-phosphate into 1,3-diphosphate. Glycolysis inhibition by 3-BrP in turn depletes the energy stores as decreased amounts of glucose can be converted into the end product, leading to cell death because of energy depletion [17,25].

Combining two drugs with different but closely related mechanisms of action can result in a synergistic combination, whereby less of each compound is needed to yield the appropriate and selective cancer-killing properties. By combining the glycolysis inhibitor, 3-BrP, and the BRD-4 inhibitor, ITH-47, synergism may be attained by simultaneously inhibiting glycolysis with 3-BrP and knocking out c-myc's capability to upregulate glycolysis with ITH-47. A further purpose was to elucidate the mechanism of action of 3-BrP, ITH-47, and the synergistic combination of these compounds on the U937 cells using various techniques including spectrophotometry, flow cytometry, and quantitative qRT-PCR.

Materials and methods

Materials

The myeloid leukemia (U937) (American Tissue Culture Collection, Maryland, USA) cell line was derived from a pleural effusion of human myeloid lymphocyte and is nonadherent under standard cell culturing methods. The antiglycolytic compound, 3-BrP, was manufactured by Sigma-Aldrich Chemical Co. (St. Louis, Missouri, USA). ITH-47 is derived from the synthesis code from iThemba Pharmaceuticals (Modderfontein, South Africa) ITH003247 and synthesized as described in Deepak *et al.* [26]. Iscove's modified Dulbecco's medium, penicillin, streptomycin, fungizone, 3,3′-dihexyloxacarbocyanine iodide, 2,7-dichlorofluorescein diacetate, and anti-c-Myc antibodies that were used in the study were manufactured by Sigma-Aldrich Chemical Co. Sterile cell culture flasks and plates were procured from Lasec (Pretoria, South Africa). The fetal bovine serum was manufactured by Biochrom (Berlin, Germany). Fluorescein isothiocyanate (FITC)-conjugated Annexin-V and FITC-anti-p53 were produced by Biolegend (San Diego, California, USA). The Phospho-Bcl-2 (Ser70) antibody used was manufactured by Cell Signaling

Technology (Beverly, Massachusetts, USA). Housekeeping gene primers including β-actin (*ACTB*), cyclin-dependent kinase inhibitor 1, or CDK-interacting protein 1 (*CDKN1A*), and β-2 microglobulin (*B2M*), as well as test primers for *p53*, *Bcl-2*, and *c-Myc* were purchased from Qiagen (Venlo, the Netherlands). Qiagen's Plant Mini Kit, PCR Clean-up kit, and RNase-free DNase were used for RNA extraction and Qiagen's QuantiTect SYBR Green RT-PCR Kit was used for qRT-PCR gene expression studies. All other chemicals (unless specified otherwise) were of analytical grade and were purchased from Sigma-Aldrich Chemical Co.

Software and docking methodology

Molecular modeling was performed on an Ubuntu 14.04 LTS system with an Intel Xeon E3-1230 V2 with a GeForce GTX 660Ti. Chimera was used for visualization and depictions [27]. For ligands, Chemsketch was used to draw two-dimensional structures with simplified molecular-input line-entry system annotations [28]. The simplified molecular-input line-entry system annotations were converted into three-dimensional structures using Open Babel 2.3.2 [29] and balloon [30,31]. Drug-likeness properties such as Lipinski and QED parameters [32] were monitored with DruLiTo (NIPER, SRS Nagar, India). Autodock Vina [33] was used to dock the ligands into receptors. An ensemble docking study was carried out with various benzotriazepine or benzodiazepine analogs bound to BRD proteins. These include BRD-2 (1) proteins 2YEK and 2YDW, the BRD-2 (2) protein 3ONI, BRD-4 (1) proteins 3MXF, 3P5O, 3U5L, 4LRG, 4F3I, and 2YEL, and the BRD-4 (2) protein 2YEM. In Autodock Vina, the exhaustiveness was set to 15, with the rest of the parameters set on default [33]. The lowest energy conformation for each from each docking suite was selected and the root-mean-square deviation (RMSD) of the crystal pose and docked pose was calculated using the match module in chimera [27]. Various test ligands with optimized drug likeness were docked into all the receptors and the lowest energy conformation for each from each of the BRD-2 (1), BRD-2 (2), BRD-4 (1), and BRD-4 (2) receptors was selected.

Ligand-binding assay

A chemiluminescent α-screen binding assay was performed by Reaction Biology Corp. (Malvern, Pennsylvania, USA) to determine the half-maximal inhibitory concentration (IC_{50}) of each compound against BRD-containing protein 2 domain 1 and 2 and bromodomain-containing protein 4 domain 1 and 2. The assay monitors the competitive displacement of a biotinylated histone H4 peptide (residues 1 – 21) containing KAc (K5/8/12/16Ac) from the BRD proteins.

Cell culture

U937 leukemia cancer cells were cultured in Iscove's modified Dulbecco's medium and supplemented with 10% heat-inactivated fetal calf serum (56°C, 30 min), 100 U/ml penicillin G, 100 μg/ml streptomycin, and fungizone (250 μg/l). ITH-47 was dissolved in dimethyl sulfoxide. The final concentration of dimethyl sulfoxide did not exceed 0.05% in cell culture. Experiments were conducted in 24-well, six-well plates, or 25 cm^2 cell culture flasks. Exponentially growing cells were seeded at 5000, 50 000, and 250 000 cells/well for 96-well, 24-well, and six-well plates, respectively. Cells were seeded at 750 000 cells/25 cm^2 cell culture flask.

Cell growth

Cell quantification was performed using the Luna-II automated cell counter (Logos Biosystems Inc., Annandale, Virginia, USA) (i). The Luna-II system uses the principles of the dye exclusion method, with trypan blue as the stain. Trypan blue selectively stains dead cells, whereas viable cells are excluded as intact cell membranes prevent dye absorption (ii). The values of total cell count for viable cells were then recorded to determine the IC_{50} of ITH-47 and 3-BrP. The IC_{50} was determined when:

$$IC_{50}=\frac{\text{Number of viable cells exposed to test condition}}{\text{Number of viable cells exposed to vehicle treated control}}\times 100=50\,\%\,.$$

At least three biological repeats, each with three technical repeats, were performed to obtain a minimum total of repeats of 9 ($n=9$). From the cell growth analysis, the concentration at which ITH-47 and 3-BrP inhibited growth by 50% was selected as an IC_{50}, and was used at a constant concentration throughout the rest of the experiments. The IC_{50} of each compound was used in the combination index (CI) equation to determine whether synergy occurred when a CI value was less than 1. The Loewe additivity measures the effects of compounds when used in combination, with the principle that similar drugs will have an additive effect of double the dose [34]. If a combination of compounds were to have a synergy, the combinations of these compounds are to be less than the dosage needed for the same effect in the compounds alone [34]. The IC_{50} of ITH-47 and 3-BrP were first determined by the cell growth study. To determine whether a synergistic effect occurred between ITH-47 and 3-BrP, a combination index study was carried out. The CI was determined using the CI equation [35]:

$$CI=\frac{A}{A_{50}}+\frac{B}{B_{50}},$$

where A is the concentration of ITH-47 in combination with B that yields IC_{50}; B is the concentration of 3-BrP in combination with A that yields IC_{50}; A_{50} is the IC_{50} of ITH-47; and B_{50} is the IC_{50} of 3-BrP.

Flow cytometry

Flow cytometry was used to measure the DNA content, apoptosis, mitochondrial membrane potential, redox status, and protein expression of c-myc, ser70 phosphorylated Bcl-2, and p53 for exposed and control U937 leukemia cells. Propidium iodide was used to stain the nucleus to determine the amount of DNA present. A FITC-conjugated Annexin-V antibody was used to measure the translocation of the membrane phosphatidylserine as an indication of apoptosis. To study the effects of oxidative stress, a cell-permeable and non-fluorescent probe, 2,7-dichlorofluorescein diacetate, was used to indicate the hydrogen peroxide (H_2O_2) generation within the cells. 2,7-Dichlorofluorescein diacetate is de-esterified intracellularly and transforms into the highly fluorescent derivative 2,7-dichlorofluorescein upon oxidation [36]. The differences in mitochondrial membrane potential (depolarization) were measured with 3,3′-dihexyloxacarbocyanine iodide [$DiOC_6$ (3)]. $DiOC_6$ (3) is a dye with cationic properties that accumulated and collected in the polarized mitochondria of viable cells to fluoresce as a bright green light [37]. The dye is unable to aggregate when mitochondrial membrane potential is lost, resulting in the dye remaining in the cytoplasm with decreased green fluorescence [38]. FITC-conjugated anti-p53, FITC-conjugated anti-phospho-Bcl-2 (Ser70) antibody, and FITC-conjugated anti-c-myc antibodies were used to measure the expression of these proteins in cells. Data from at least 10 000 cells were captured with the FC-500 flow cytometer (Beckman Coulter South Africa (Pty) Ltd, South Africa) or the BD-Accuri C6 Plus (BD Biosciences, Franklin Lakes, New Jersey, USA) flow cytometer. For the FC-500 flow cytometer, red emissions of 620 nm for propidium iodide were detected with the FL-3 filter and green emissions of 525 nm for FITC-conjugated antibodies were detected with the FL-1 filter. For the BD-Accuri C6 Plus, the FL-1 filter was used to detect the FITC-conjugated anti-phospho-Bcl-2 (Ser70) antibody. Data were analyzed using WEASEL, version 3.0 software (F. Battye, Walter and Eliza Hall Institute, Melbourne, Victoria, Australia). Detailed methods are presented in Supplementary Information S1 (Supplemental digital content 1, *http://links.lww.com/ACD/A250*).

Gene expression quantification: reverse transcription quantitative polymerase chain reaction of c-Myc, Bcl-2, and p53

Examination of the gene expression of c-myc, Bcl-2, and p53 genes was performed using quantitative reverse transcriptase PCR (qRT-PCR) to gain an insight into the mechanism of action of 3-BrP, ITH-47, and the synergistic combination. qRT-PCR is the enzymatic amplification of a fragment mRNA between a pair of primers; the technique offers an accurate measurement of the mRNA level, which correlates to the quantification the expression of the gene of interest. RNA was extracted using Qiagen's RNeasy spin column. A one-step RT-PCR using Qiagen's QuantiTect SYBR Green RT-PCR Kit was performed. Three housekeeping genes, a genomic DNA control, positive PCR control, and reverse transcription controls were included. The data obtained were analyzed using Roche LightCycler Nano, version 1.0.7 software, where the C_q values were obtained. The relative gene expression levels were calculated and analyzed using the $2^{-\Delta\Delta C_t}$ method [39]. Detailed methods are presented in Supplementary Information S1 (Supplemental digital content 1, *http://links.lww.com/ACD/A250*).

Statistical analysis

Data are representative of three independent experiments unless otherwise stated and are represented as mean ± SD. Statistical analysis was carried out by one-way analysis of variance, followed by Tukey's post-hoc multiple comparison test using GraphPad Prism Software (GraphPad Software Inc., San Diego, California, USA). Measurement of fluorescence by flow cytometry was expressed as a ratio of the value measured for vehicle-treated exposed cells (relative fluorescence). P less than 0.05 was considered statistically significant.

Results

Docking

An ensemble docking method was used to take into account minor structural variations of receptors under different conditions. Only BRD-2 and BRD-4 receptors with Bzt or Bzd ligands bound to them were included. The rationale behind this is that these receptor configurations are likely to be the most accurate representations for the Bzt compounds being designed in this project. The conserved water molecules in the acetyl-lysine (AcK) binding pocket were retained during receptor preparation as they play a crucial role in the binding of various compounds to BRD-2 and BRD-4 proteins [40,41]. Autodock Vina was used to observe whether docking can reproduce the binding poses of the ligands of the original radiographic structures. Autodock Vina was good at reproducing the radiographic ligand structures, with 80% of the redocked poses having an RMSD of less than 1.5, indicating that the software can reproduce the original binding mode and is thus reliable to identify new compounds capable of binding to BRD-4 (Fig. 1a). The weakest binding energy for Autodock Vina was − 9.2 kcal/mol (3MXF) (Fig. 1a); therefore, the new compounds to be synthesized had to have at least one binding energy better than this. A further criterion was that the binding energy of a particular compound would be more selective toward the BRD-4 receptors compared with the BRD-2 receptors (Fig. 1a). The docking poses were also inspected to ensure that the compounds occupy the AcK-binding site and that the diazolo group of the compounds interacts with ASN99 (Fig. 1b). On the basis of these criteria, ITH-47 was synthesized by iThemba Pharmaceuticals (Modderfontein, Gauteng, South Africa)

Fig. 1

(a)

Recepetor-ligand	Autodock Vina	
	Binding Energy	RMSD
2YDW BRD2(1)	-10.4	1.11
2YEK BRD2(1)	-10.6	1.52
3ONI BRD2(2)	-9.6	0.96
2YEL BRD4(1)	-10.0	1.68
3MXF BRD4(1)	-9.4	0.37
3P5O (BRD4(1)	-9.8	1.40
3U5L BRD4(1)	-10.0	0.51
4F3I BRD4(1)	-9.2	0.65
4LRG BRD4(1)	-9.8	1.01
2YEM BRD4(2)	-10.1	1.78

Ligand	BRD2_1	BRD2_2	BRD4_1	BRD4_2
ITH-47	-9.40	-8.60	-9.60	-8.90

(b)

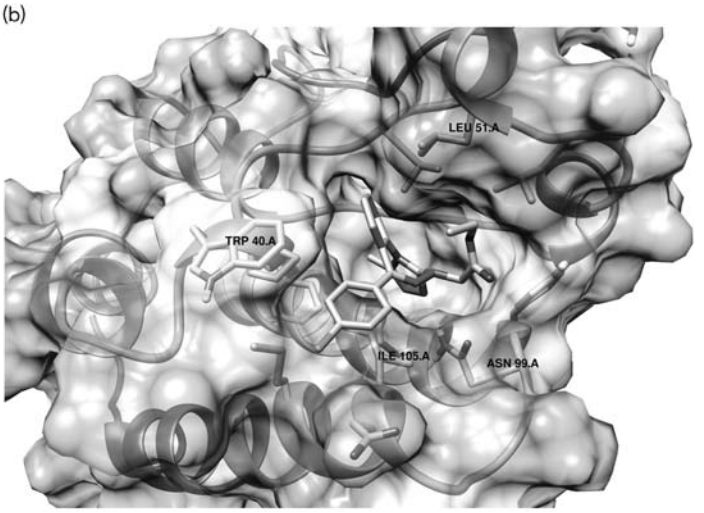

Binding energies and pose of ITH-47. (a) Binding energies of benzotriazepine and benzodiazepine analogs using Autodock Vina. Autodock Vina could reproduce the radiographic ligand structures (RMSD < 2) for all the structures. ITH-47 has better binding energies for BRD-4 proteins compared with BRD-2 proteins and was chosen for synthesis. (b) ITH-47 docked into BRD-4 (1), showing key interactions including a hydrogen bond interaction between TH-47 and ASN99. RMSD, root-mean-square deviation.

and, later, more of the compounds were synthesized by WuXi AppTec (Shanghai, China) [26]. All compounds were more than 95% pure.

Ligand-binding

To determine whether ITH-47 binds to and inhibits BRD-2 and BRD-4 proteins and whether ITH-47 is selective against BRD-4 proteins [both BRD-4 (1) and BRD-4 (2)] compared with BRD-2 [both BRD-2 (1) and BRD-2 (2)], a chemiluminescent α-screen binding assay was performed by Reaction Biology Corp. using a tandem BRD-4 and BRD-2 construct. The concentration of JQ1 needed to displace 50% of biotinylated histone H4 peptide (residues 1–21) containing KAc (K5/8/12/16Ac) from the tandem BRD-4 proteins was 75 and 55 nmol/l for the tandem-BRD-2 protein (Fig. 2a and b). This is within the range from other studies and suggests that there is no selectivity toward BRD-4 compared with BRD-2 for JQ1. ITH-47 was 2.2× more selective against the cancer-associated BRD-4 (490 nmol/l) protein compared to BRD-2 (1120 nmol/l) (Fig. 2a and b). Although the compound does not appear to be as potent as JQ1, it is more selective at inhibiting the BRD-4 protein compared with BRD-2, which satisfied the main aim of designing this compound, and is also beneficial for selectively targeting the cancer-associated BRD-4 proteins.

Cell growth and combination index

Cell growth studies using the Luna-II automated cell counter enabled the accurate quantification of U937 cells. Data captured from the Luna-II system were analyzed and each test condition's viable cell numbers were adjusted to a percentage ratio compared with the vehicle control with vehicle-control set to 100%. Data were analyzed in a graphic representation of the effects of ITH-47 on cell growth on the U937 cells. Cells exposed to the lowest concentration of ITH-47 (0.5 μmol/l) yielded a number of viable cells relative to the vehicle-treated control of 74%, whereas the highest exposed concentration, 5 μmol/l, was only 18% (Fig. 3a). ITH-47 inhibited cell growth at a percentage expressed ratio to the vehicle control of 50% at a concentration of 2 μmol/l (Fig. 3a). A concentration range of 2.5, 5, 6, and 7.5 μmol/l was chosen to determine the IC_{50}. At the lowest selected concentration of 3-BrP (2.5 μmol/l), the number of viable cells compared with the vehicle-treated control was 68%, 62% at 5 μmol/l, 52% at 6 μmol/l, and 21% at 7.5 μmol/l (Fig. 3b). Therefore, in this study, 3-BrP inhibited cell growth at percentage expressed ratio to the vehicle control of 50% at a concentration of 6 μmol/l (Fig. 3b).

Initial studies with a CI lower than 0.8 showed no synergism (data not shown). It was decided to maintain the concentrations of ITH-47 constant and increase the concentrations of 3-BrP in fractions to obtain a CI that is equal to 0.8 and 0.9 (Fig. 3c). It was found that combination 5 with a CI of 0.8 reduced growth 60.90% of the control, whereas combination 10 led to a 50% growth inhibition (Fig. 3d). Even though combination 6 reduced cell growth to 46%, there was no statistically significant difference between combinations 6 and 10 (Fig. 3d). Combination 9 showed the best effect on cell growth (33.75%); however, these results could not be repeated

Fig. 2

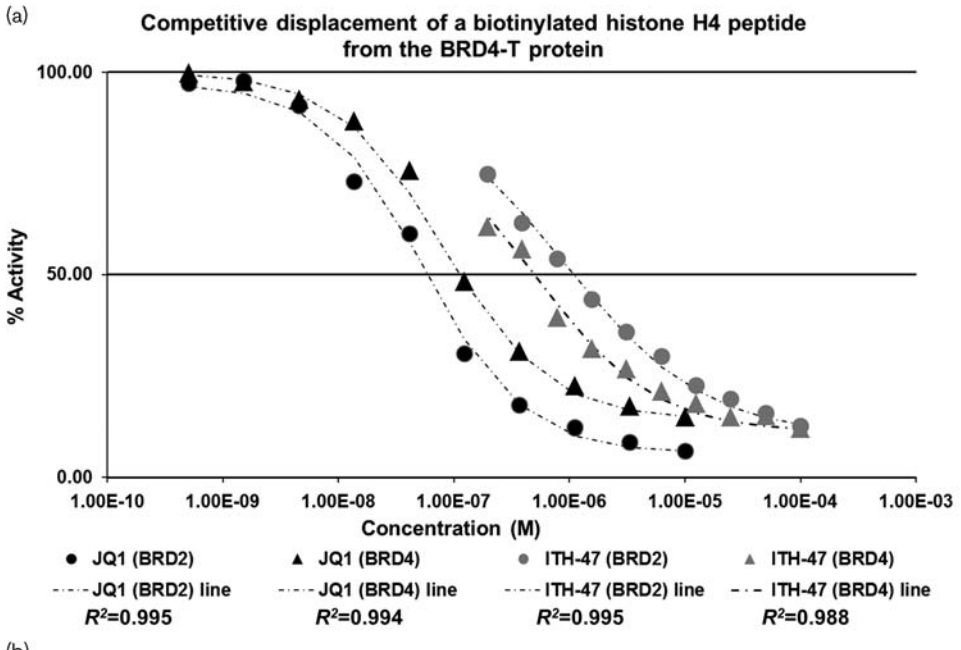

(b)

Compound ID	Compound IC_{50} (μM)		Selectivity towards inhibiting BRD4
	BRD2-T	BRD4-T	
ITH-47	1.12	0.49	2.28
JQ-1	0.055	0.075	0.73

Bzt-ITH-47 inhibition of tandem BRD-2 and tandem BRD-4. ITH-47 is 2.28 times more selective toward BRD-4 compared with BRD-2.

independently (data not shown) (Fig. 3d). Combination 10 was reliable in reducing cell viability to 50% compared with the control, and was thus used in all subsequent mechanistic studies. To demonstrate that the synergistic concentration was more potent than the concentration of these compounds on their own, cells were exposed to ITH-47 (1 μmol/l) and 3-BrP (2.4 μmol/l). The growth inhibition of ITH-47 (1 μmol/l) inhibited the growth of the U937 cells by 70% and 3-BrP (2.4 μmol/l) inhibited the growth by only 68% (Fig. 3e). When the U937 cells were exposed to the compounds alone, the cell growth inhibition was less than when the U937 cells were exposed to the compounds together. This novel finding indicates a synergistic effect of the combination of ITH-47 and 3-BrP on cell growth.

Cell cycle, apoptosis, mitochondrial membrane potential, and redox status

Cell cycle analyses showed that an increase in the number cells in the sub-G_1 phase of the cell cycle was observed in cells exposed to compounds (Fig. 4a and b). There was also an increase in the S phase in U937 cells exposed to 3-BrP and the combination (Fig. 4a and b). The increase in the sub-G_1 fraction suggests that the compounds can induce apoptosis. Apoptosis induction was confirmed with the Annexin-V assay. Viable cell numbers in ITH-47-exposed samples decreased statistically significantly to 73.4%; 18.2% were found to be early apoptotic cells and 7.42% of the sample's cells were late apoptotic cells, and only 0.95% of cells were found to be necrotic (Fig. 4c and d). 3-BrP also affected viable cell numbers (73.7%) and increased apoptotic cell numbers to 17.7% in early apoptosis and 5.29% in late apoptosis (Fig. 4c and d). Synergistic combination exposure decreased viable cell numbers to similar percentages as ITH-47 and 3-BrP to a value of 73.8% (Fig. 4c and d). It was found that the synergistic combination of the compounds increased early apoptotic cells to 18.3% and late apoptotic cells to 6.2%. Necrotic cell numbers were similar to the vehicle control, 1.78% (Fig. 4c and d), indicating cell death apoptosis and not necrosis.

To determine whether apoptosis induction occurs through the intrinsic mitochondrial pathway, mitochondrial membrane depolarization was measured. The M1 region (Fig. 5a) indicates cells with decreased green fluorescence and thus cells with increased mitochondrial membrane depolarization [42]. Only ITH-47 showed a statistically significant increase for region M1 and thus

Fig. 3

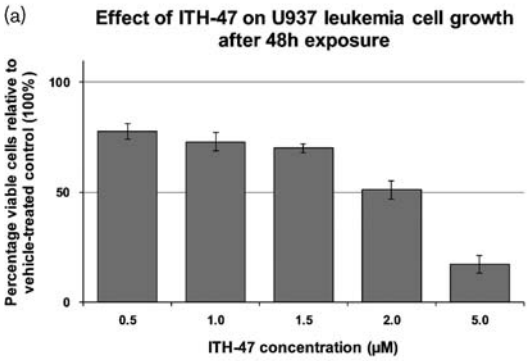

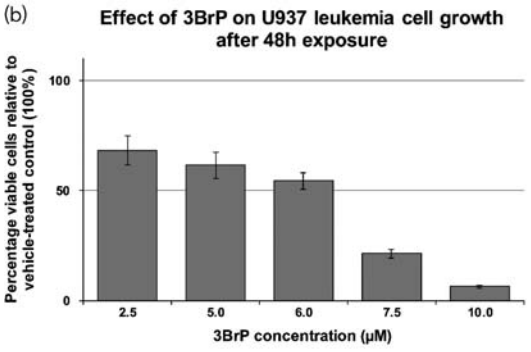

(c)

Combination Index	0.8					0.9				
Combination	1	2	3	4	5	6	7	8	9	10
ITH-47	0.6 μM	0.7 μM	0.8 μM	0.9 μM	1.0 μM	0.6 μM	0.7 μM	0.8 μM	0.9 μM	1.0 μM
3BrP	3.0 μM	2.7 μM	2.4 μM	2.1 μM	1.8 μM	3.6 μM	3.3 μM	3 μM	2.7 μM	2.4 μM
% Cell viability relative to vehicle-treated control	94.7%	73.35%	79.20%	63.03%	60.90%	45.59%	83.86%	56.57%	33.75%	50.28%

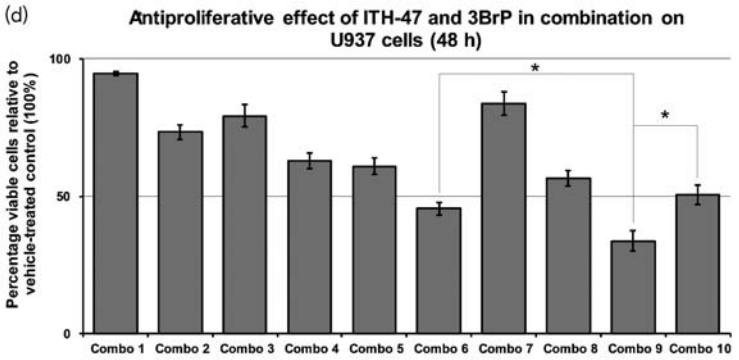

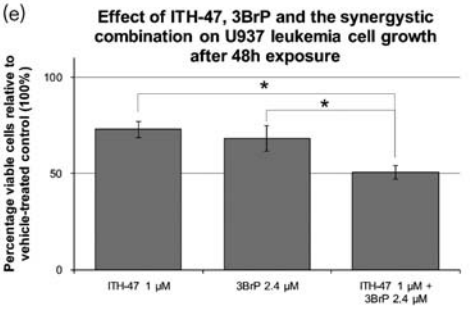

Effect of ITH-47 (a), 3-BrP (b), and combinations of ITH-47 and 3-BrP (c, d) on the cell viability of U937 cells after 48 h exposure. Cell numbers of treated cells are expressed as percentages relative to the vehicle control after 48 h exposure times. The combination is more potent than the compounds alone (e). *Indicates a *P* value less than 0.05 compared with the vehicle-treated control or between connecting lines.

Fig. 4

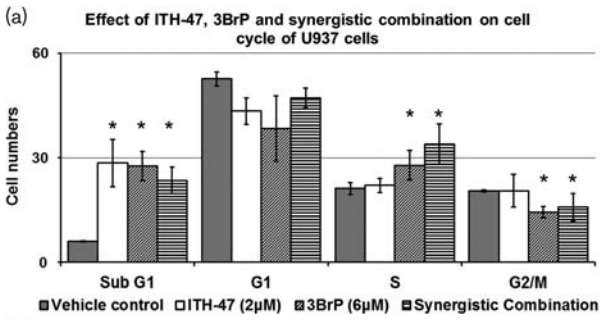

(b)

Cell cycle phase	Vehicle control (mean)	ITH-47 (2 μM) (mean)	3BrP (6 μM) (mean)	Synergistic Combination (mean)
Sub G_1	6.02	28.49	27.64	23.51
G_1	52.60	43.37	38.39	47.10
S	21.18	22.05	27.86	33.90
G_2/M	20.50	23.04	14.39	15.82

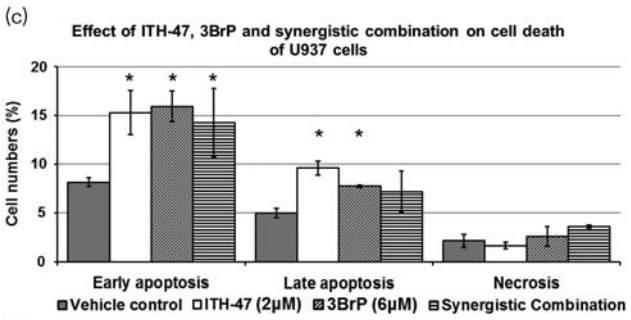

(d)

	Vehicle Control (mean)	ITH-47 (2 μM) (mean)	3BrP (6 μM) (mean)	Synergistic Combination (mean)
Viable	84.73	73.43	73.70	74.97
Early Apoptosis	8.16	15.30	15.93	14.27
Late Apoptosis	4.98	9.60	7.75	7.20
Necrosis	2.14	1.65	2.60	3.61

Graphic representation of the cell cycle progression (a, b) and apoptosis induction (c, d) for U937 cells treated with ITH-47, 3-BrP, and a synergistic combination of ITH-47 and 3-BrP. Cells exposed to compounds had an increased cell content in sub-G_1 and increased levels of apoptosis induction. *Indicates a *P* value of less than 0.05.

Fig. 5

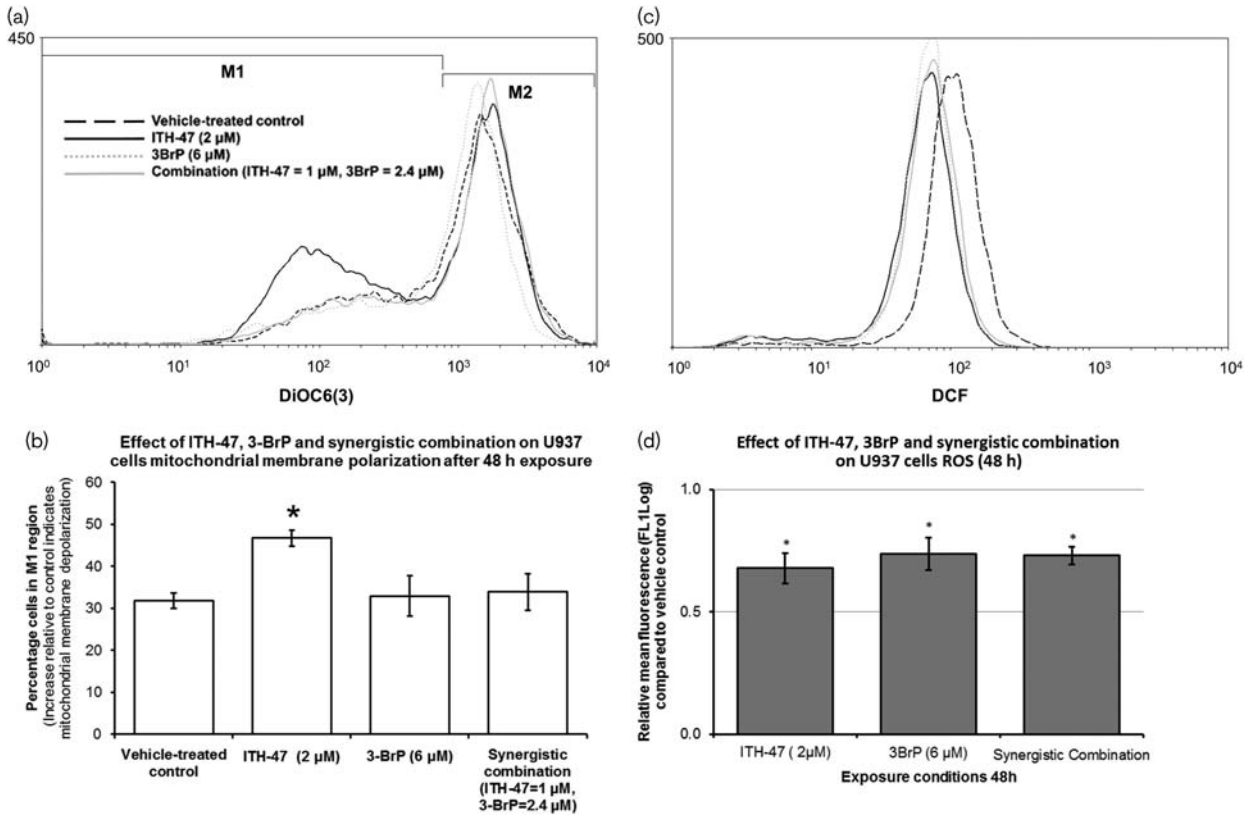

Graphic representation of data analysis of mitochondrial membrane depolarization (a, b) and reactive oxygen species (ROS) production (c, d) for U937 cells treated with ITH-47, 3-BrP, and a synergistic combination of ITH-47 and 3-BrP. An increase in the M1 region was observed for only ITH-47-treated (2 µmol/l) U937 cells after 48 h exposure (a, b). A decrease in ROS production was observed in all treated cells (c, d).*Indicates a *P* value less than 0.05 compared with the control.

increased mitochondrial membrane depolarization after 48 h exposure (Fig. 5a and b). A statistically significant decrease in reactive oxygen species (ROS) production was observed through all three test conditions (Fig. 5c and d).

Gene and protein expression of c-myc, ser70 phosphorylated Bcl-2, and p53

The level of mRNA is an indication of the gene expression level of the gene of interest. *c-Myc*, *Bcl-2*, and *p53* were selected as the genes of interest in this gene expression study. The three housekeeping genes selected were *ATC*, *CDK*, and *B2M* and the $2^{-\Delta\Delta C_t}$ method [39] was used to determine gene expression relative to the vehicle-treated control. ITH-47 treatment resulted in statistically significantly decreased expression of *c-Myc* (0.01-fold), *Bcl-2* (0.41-fold), and *p53* (0.03-fold) (Fig. 6a). A statistically significant increase in the expression of *c-myc* (1.9-fold) and *p53* (1.6-fold) was found in 3-BrP-treated cells after 48 h exposure (Fig. 6a). For the combination, only *c-myc* (0.2-fold) and *Bcl-2* (0.33-fold) were statistically significantly decreased compared with the vehicle-treated control (Fig. 6a).

Protein expression studies were carried out to determine the amount of protein levels within cells as gene expression studies take into account only the quantification of mRNA. Levels of mRNA do not necessarily correlate to protein levels in cells. Three antibodies were used to detect c-myc, Ser70 phosphorylated Bcl-2, and p53 protein expression. Exposure to ITH-47 (2 µmol/l) significantly decreased c-myc protein expression by 79% in U937 cells relative to the vehicle control (Fig. 6b). c-Myc expression was decreased to a lesser extent in the 3-BrP (6 µmol/l, 46%) and combination-treated (41%) U937 cells after 48 h exposure (Fig. 6b). ITH-47 exposure had no effect on p53 levels and only a small increase in p53 expression was observed in 3-BrP-treated (1.16-fold) and combination-treated (1.22-fold) U937 cells after 48 h exposure (Fig. 6c). The cells exposed to ITH-47, 3-BrP, and a synergistic combination showed a statistically significant decrease in the amount of ser70 phosphorylated Bcl-2 protein (Fig. 6d). Cells exposed to ITH-47 decreased these Bcl-2 proteins by 18% relative to the vehicle control, with 3-BrP also having a similar effect: 17% reduction in ser70 phosphorylated Bcl-2 levels (Fig. 6d). The synergistic combination exposure

Fig. 6

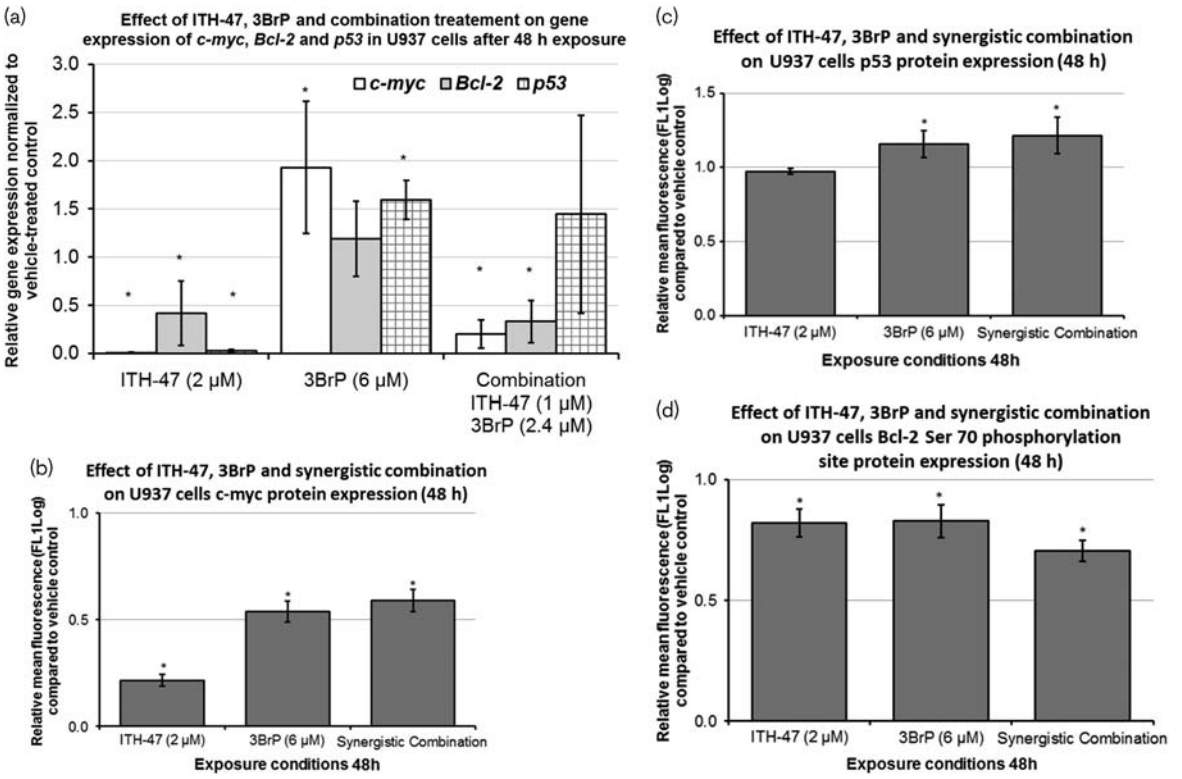

Graphic representation of the effects of test conditions on gene expression (a) and protein expression (c–d) of *Bcl-2*, *c-Myc*, and *p53* for U937 cells treated with ITH-47, 3-BrP, and a synergistic combination of ITH-47 and 3-BrP. ITH-47 decreased *c-Myc*, *Bcl-2*, and *p53* gene expression. 3-BrP increased the gene expression of both *c-myc* and *p53*. The combination of ITH-47 and 3-BrP decreased the expression of *c-Myc* and *Bcl-2* (a). A decrease in c-myc protein levels was detected in all treated samples (b). Exposure to 3-BrP and a synergistic combination increased the expression of p53 (b). All test conditions reduced the phosphorylation at the Ser70 phosphorylation site (d).

decreased the ser70 phosphorylated Bcl-2 proteins by 30% compared with the vehicle-treated control (Fig. 6d).

Discussion and conclusion

This novel study is the first to investigate the effects of a glycolytic inhibitor, 3-BrP, in combination with a BRD-4 inhibitor, ITH-47, on cell growth and cell death in U937 myeloid leukemia cells. The study focused on the mechanistic effect that the compounds had on the cell line, as well as the effect that the compounds have in combination. The cell growth studies using the Luna-II automated cell counter ensured accurate and rapid results. By using the device's principle of the Trypan blue exclusion method, it was possible to determine the effect that 3-BrP and ITH-47 had on the growth of U937 cells. Cell growth was inhibited by 50% when using a concentration of 6 µmol/l of 3-BrP and 2 µmol/l of ITH-47. Although ITH-47 appears to be less potent than JQ1 as described by Herrmann *et al.* [43], ITH-47 shows a better selectivity profile compared with JQ1. ITH-47 is 2.28 times more selective toward inhibiting BRD-4 compared with BRD-2 whereas JQ1 is more selective at inhibiting BRD-2 compared with BRD-4. A good selectivity profile is needed to ensure that the effect of the compound is due to on-target effect. This makes ITH-47 a more ideal compound to target BRD-4-sensitive cancers such as AML [44].

Several experimental results from the present study support ITH-47 as a BRD-4-inhibiting compound in live cells. Most importantly, inhibition of BRD-4 in various BRD-4-sensitive leukemic cancer cell lines is associated with decreased c-myc gene and protein expression [11,44,45]. In this study, exposure of 2 µmol/l to U937 myeloid leukemia cells resulted in a significant decrease in both gene and protein expression of the *c-myc* gene and c-myc protein. Furthermore, studies have shown that BRD-4 inhibition results in decreased ROS formation [46,47] and the present study show that ITH-47 attenuates ROS production in U937 cells after 48 exposure. The possible mechanism of action for this effect is likely because of upregulation of antioxidant proteins as described by Michaeloudes *et al.* [47]. Finally, BRD-4 inhibition in c-myc-sensitive leukemic cancers results in the induction of apoptosis [11,41,44,48,49] and the present study shows that apoptosis is induced. The data suggest that apoptosis is likely induced by the intrinsic

mitochondrial as ITH-47 causes decreased expression of ser70 phosphorylated Bcl-2, which in turn plays a role in inducing the observed mitochondrial membrane depolarization in ITH-47-treated U937 cells.

The IC_{50} for 3-BrP after 48 h exposure was 6 μmol/l in the present study and this concentration was sufficient to induce apoptosis. However, no changes in the mitochondrial membrane potential were observed, suggesting that apoptosis was induced by a pathway other than the intrinsic mitochondrial pathway. Ganapathy-Kanniappan *et al.* [50] showed that 3-BrP treatment of human hepatocellular carcinoma cells resulted in endoplasmic reticulum (ER) stress and apoptosis. Yu *et al.* [51] also showed that hexokine II inhibition results in the ER-mediated apoptosis. 2-deoxyglucose, another anti-glycolytic compound, is can induce ER-mediated apoptosis [52,53]. Therefore, a potential pathway for apoptosis induction in response to 3-BrP in U937 cells is the intrinsic endoplasmic reticulum pathway; however, this needs to be tested in future studies. 3-BrP treatment of U937 cells resulted in abrogated ROS production and c-myc expression. Both increased ROS and increased c-myc expression can activate several progrowth pathways [9,54,55]. It is therefore reasonable to conclude that the 3-BrP can reduce cell growth because of its anti-glycolytic, ROS-reducing, and c-myc-lowering effect. The exact mechanism through which 3-BrP reduces ROS and c-myc expression remains to be elucidated.

ITH-47 and 3-BrP therefore appear to activate different pathways to reduce cell proliferation and induce cell death in U937 cells. In the present study, it was found that 50% of the IC_{50} of ITH-47 (1 μmol/l) and 40% of the IC_{50} of 3-BrP (2.4 μmol/l) were sufficient to reduce cell viability to 50% compared with the control. This yields a CI of 0.9. A CI of less than 1, which is indicative of synergy, CI of 1 is an additive effect, and CI more than 1 is an antagonistic effect [35]. This synergistic combination was used in subsequent mechanistic studies. Cell cycle analyses indicated that the synergistic combination increased the sub-G_1 fraction, which likely induced cell death by apoptosis. Flow cytometry analysis of Annexin-V expression confirmed apoptosis in U937 cells exposed to the synergistic combination. The combination treatment resulted in a significant reduction of *c-myc* gene expression and close to half a reduction in c-myc protein expression. The decrease in *c-myc* expression is similar to that of ITH-47 treatment, suggesting that *c-myc* gene expression downregulation was a result of ITH-47 treatment in the combination and not the 3-BrP. Similar to 3-BrP-treated cells and unlike the ITH-47-treated cells, the combination-treated cells did not result in mitochondrial membrane depolarization. Interestingly, both 3-BrP-treated and combination-treated cells showed an increase in p53 protein expression, whereas ITH-47-treated cells showed no difference in p53 protein expression. These results suggest that cell death in the combination treatment occurs in a manner similar to the 3-BrP-treated cells.

U937 cells exposed to the test conditions did not show an increase in ROS production. ROS was therefore an unlikely cause of oxidative stress-induced apoptosis. Macchioni *et al.* [56] studied the effect of 3-BrP on ROS production and found that the compound had a limited effect on cancerous cells. The decrease in ROS production may have contributed toward the decrease in the proliferation of the cells as elevated ROS levels have been linked to the progression of AML cells [57].

Conclusion

An antiglycolytic compound, 3-BrP, and a novel BRD inhibitor, ITH-47, inhibited cell growth and increased cell death *in vitro*. The concentrations to obtain an IC_{50} when both compounds were used in combination were lower than when the cells were exposed to the compounds individually. This provides insightful new knowledge of the mechanism of action of ITH-47 and the combination of 3-BrP and ITH-47. A lower dosage of compounds may lead to fewer side effects and the pathway-specific action of the compounds may lead to a more efficient targeted therapy to help vulnerable patients overcome AML. As Tallarida [35] stated in his article, there is a growing awareness of the use of compounds in a combination that has a synergistic effect to treat cancer and can lead to lower dosage as well as a decrease in adverse effects. 3-BrP and ITH-47 can target different pathways in causing cell death and thereby can contribute toward increased efficacy of a combination targeted therapy. This research provides a basis for future research to find more efficient and less harmful therapy in AML patient with cancerous cells that have increased chemo-resistance.

Acknowledgements

Conflicts of interest

None declared.

References

1 Jemal A, Center MM, Ferlay J, Ward E, Forman D. Global Cancer Statistics. *Am Cancer Soc* 2011; **61**:2.
2 Ferlay J, Soerjomataram I, Dikshit R, Eser S, Mathers C, Rebelo5 M, *et al.* Cancer incidence and mortality worldwide: Sources, methodsand major patterns in GLOBOCAN 2012. *Int J Cancer* 2015; **136**:359–386.
3 Herbst MC. *Fact sheet on adult acute myeloid leukaemia.* Africa: CAoS; 2016.
4 American Cancer Society. Current Grants by Cancer Type 2016. Available at: *http://www.cancer.org/research/currentlyfundedcancerresearch/grants-by-cancer-type.* [Accessed 18 November 2016].
5 Wiernik PH. In: Goldman JM, Gordon MY, editors. *Neoplastic diseases of the blood.* Cambridge: Cambridge University Press; 2003. pp. 3–4.
6 Travis LB, Li CY, Zhang ZN. Hematopoietic malignancies and related disorders among benzene-exposed workers in China. *Leuk Lymphoma* 1994; **14**:91–102.
7 Klug WS, Cummings MR, Spencer CA, Palladino MA. *Concepts of genetics*, 9th ed. San Fransisco: Pearson Education; 2009.
8 Estey E, Hartmut D. Acute myeloid leukaemia. *Lancet* 2006; **368**:1894–1907.

9 Lee GY, Christina S, Tien SL, Ghafar ABA, Hwang W, Lim LC, *et al*. Acute promyelocytic leukemia with PML-RARA fusion on i (17q) and therapy-related acute myeloid leukemia. *Cancer Genet Cytogenet* 2005; **159**:129–136.
10 Dang CV, Le A, Gao P. MYC-induced cancer cell energy metabolism and therapeutic opportunities. *Clin Cancer Res* 2009; **15**:6479–6483.
11 Filippakopoulos P, Qi J, Picaud S, Shen Y, Smith WB, Fedorov O, *et al*. Selective inhibition of BET bromodomains. *Nature* 2010; **468**:1067–1073.
12 Nesbit CE, Tersak JM, Prochownik EV. MYC oncogenes and human neoplastic disease. *Oncogene* 1999; **18**:3004–3016.
13 Pelengaris S, Khan M, Evan G. c-MYC: more than just a matter of life and death. *Nat Rev Cancer* 2002; **2**:764–776.
14 Renneville A, Roumier C, Biggio V, Nibourel O, Boissel N, Fenaux P, *et al*. Cooperating gene mutations in acute myeloid leukemia: a review of the literature. *Leukemia* 2008; **22**:915–931.
15 Osthus RC, Shim H, Kim S, Li Q, Reddy R, Mukherjee M, *et al*. Deregulation of glucose transporter 1 and glycolytic gene expression by c-Myc. *J Biol Chem* 2000; **275**:21797–21800.
16 Warburg O. *Ueber den stoffwechsel der tumoren*. London: Constablr; 1930. pp. 309–313.
17 Cardaci S, Desideri E, Ciriolo MR. Targeting aerobic glycolysis: 3-bromopyruvate as a promising anticancer drug. *J Bioenerg Biomembr* 2012; **44**:17–29.
18 Herst PM, Howman RA, Neeson PJ, Berridge MV, Ritchie DS. The level of glycolytic metabolism in acute myeloid leukemia blasts at diagnosis is prognostic for clinical outcome. *J Leukoc Biol* 2011; **89**:51–55.
19 Chen W-L, Wang J-H, Zhao A-H, Xu X, Wang Y-H, Chen T-L, *et al*. A distinct glucose metabolism signature of acute myeloid leukemia with prognostic value. *Blood* 2014; **124**:1645–1654.
20 Bustamante E, Pedersen PL. High aerobic glycolysis of rat hepatoma cells in culture: role of mitochondrial hexokinase. *Proc Natl Acad Sci* 1977; **74**:3735–3739.
21 Nakano A, Miki H, Nakamura S, Harada T, Oda A, Amou H, *et al*. Up-regulation of hexokinaseII in myeloma cells: targeting myeloma cells with 3-bromopyruvate. *J Bioenerg Biomembr* 2012; **44**:31–38.
22 Dey A, Nishiyama A, Karpova T, McNally J, Ozato K. Brd4 marks select genes on mitotic chromatin and directs postmitotic transcription. *Mol Biol Cell* 2009; **20**:4899–4909.
23 Campbell M, Farrell S. *Biochemistry*, 6th ed. Belmont: Brooks/Cole; 2008. pp. 493–495.
24 Koa YH, Smitha BL, Wanga Y, Pompera MG, Rinic DA, Torbensond MS, *et al*. Advanced cancers: eradication in all cases using 3-bromopyruvate therapy to deplete ATP. *Biochem Biophys Res Commun* 2004; **324**:269–275.
25 Ganapathy-Kanniappan S, Vali M, Kunjithapatham R, Buijs M, Syed LH, Rao PP, *et al*. 3-Bromopyruvate: A new targeted antiglycolytic agent and a promise for cancer therapy. *Curr Pharm Biotechnol* 2010; **11**:510–517.
26 Deepak V, Wang B, Koot D, Kasonga A, Stander XX, Coetzee M, *et al*. In silico design and bioevaluation of selective benzotriazepine BRD4 inhibitors with potent antiosteoclastogenic activity. *Chem Biol Drug Des* 2017; **90**:1–161.
27 Pettersen EF, Goddard TD, Huang CC, Couch GS, Greenblatt DM, Meng EC, *et al*. UCSF Chimera – a visualization system for exploratory research and analysis. *J Comput Chem* 2004; **25**:1605–1612.
28 Acdlabs.com. *Advanced Chemistry Development, Inc*, 12.0 ed. Toronto, Canada: ACD/Chemsketch; 2015.
29 OLBoyle NM, Banck M, James CA, Morley C, Vandermeersch T, Hutchison GR. Open Babel: an open chemical toolbox. *J Cheminform* 2011; **3**:33.
30 Vainio MJ, Johnson MS. Generating conformer ensembles using a multiobjective genetic algorithm. *J Chem Inf Model* 2007; **47**:2462–2474.
31 Puranen JS, Vainio MJ, Johnson MS. Accurate conformation-dependent molecular electrostatic potentials for high-throughput in silico drug discovery. *J Comput Chem* 2010; **31**:1722–1732.
32 Bickerton GR, Paolini GV, Besnard J, Muresan S, Hopkins AL. Quantifying the chemical beauty of drugs. *Nat Chem* 2012; **4**:90–98.
33 Trott O, Olson AJ. AutoDock Vina: improving the speed and accuracy of docking with a new scoring function, efficient optimization, and multithreading. *J Comput Chem* 2010; **31**:455–461.
34 Berenbaum M. Synergy, additivism and antagonism in immunosuppression - critical review. *Clin Exp Immunol* 1977; **28**:1–18.
35 Tallarida RJ. Quantitative methods for assessing drug synergism. *Genes Cancer* 2011; **2**:11.
36 Andreyev AY, Kushnareva YE, Starkov AA. Mitochondrial metabolism of reactive oxygen species. *Biochemistry* 2005; **70**:200–214.
37 Guthrie H, Welch G. Determination of high mitochondrial membrane potential in spermatozoa loaded with the mitochondrial probe 5,5′,6,6′-tetrachloro-1,1′,3,3′-tetraethylbenzimidazolyl-carbocyanine iodide (JC-1) by using fluorescence-activated flow cytometry. *Methods Mol Biol* 2008; **477**:89–97.
38 Chang H, Huang H, Huang T, Yang P, Wang Y, Juan H. Flow cytometric detection of mitochondrial membrane potential. *Bioprotocol* 2013; **3**:8.
39 Livak KJ, Schmittgen TD. Analysis of relative gene expression data using real-time quantitative PCR and the $2-\Delta\Delta CT$ method. *Methods* 2001; **25**:402–408.
40 Cheng T, Li Q, Zhou Z, Wang Y, Bryant SH. Structure-based virtual screening for drug discovery: a problem-centric review. *AAPS J* 2012; **14**:133–141.
41 Chung C-W, Coste H, White JH, Mirguet O, Wilde J, Gosmini RL, *et al*. Discovery and characterization of small molecule inhibitors of the BET family bromodomains. *J Med Chem* 2011; **54**:3827–3838.
42 Chang H-Y, Huang H-C, Huang T-C, Yang P-C, Wang Y-C, Juan H-F. Ectopic ATP synthase blockade suppresses lung adenocarcinoma growth by activating the unfolded protein response. *Cancer Res* 2012; **72**:4696–706.
43 Herrmann H, Blatt K, Shi J, Gleixner KV, Cerny-Reiterer S, Müllauer L, *et al*. Small-molecule inhibition of BRD4 as a new potent approach to eliminate leukemic stem- and progenitor cells in acute myeloid leukemia (AML). *Oncotarget* 2012; **3**:12.
44 Zuber J, Shi J, Wang E, Rappaport AR, Herrmann H, Sison EA. RNAi screen identifies Brd4 as a therapeutic target in acute myeloid leukaemia. *Nature* 2011; **478**:524–528.
45 Coudé M-M, Braun T, Berrou J, Dupont M, Bertrand S, Masse A, *et al*. BET inhibitor OTX015 targets BRD2 and BRD4 and decreases c-MYC in acute leukemia cells. *Oncotarget* 2015; **6**:17698.
46 Hussong M, Börno S, Kerick M, Wunderlich A, Franz A, Sültmann H, *et al*. The bromodomain protein BRD4 regulates the KEAP1/NRF2-dependent oxidative stress response. *Cell Death Dis* 2014; **5**:e1195.
47 Michaeloudes C, Mercado N, Clarke C, Bhavsar PK, Adcock IM, Barnes PJ, *et al*. Bromodomain and extraterminal proteins suppress NF-E2-related factor 2-mediated antioxidant gene expression. *Jo Immunol* 2014; **192**:4913–4920.
48 Dawson MA, Prinjha RK, Dittmann A, Giotopoulos G, Bantscheff M, Chan W-I, *et al*. Inhibition of BET recruitment to chromatin as an effective treatment for MLL-fusion leukaemia. *Nature* 2011; **478**:529–533.
49 Ott CJ, Kopp N, Bird L, Paranal RM, Qi J, Bowman T, *et al*. BET bromodomain inhibition targets both c-Myc and IL7R in high-risk acute lymphoblastic leukemia. *Blood* 2012; **120**:2843–2852.
50 Ganapathy-Kanniappan S, Geschwind J-FH, Kunjithapatham R, Buijs M, Syed LH, Rao PP, *et al*. 3-Bromopyruvate induces endoplasmic reticulum stress, overcomes autophagy and causes apoptosis in human HCC cell lines. *Anticancer Res* 2010; **30**:923–935.
51 Yu SJ, Yoon J-H, Yang J-I, Cho EJ, Kwak MS, Jang ES, *et al*. Enhancement of hexokinase II inhibitor-induced apoptosis in hepatocellular carcinoma cells via augmenting ER stress and anti-angiogenesis by protein disulfide isomerase inhibition. *J Bioenerg Biomembr* 2012; **44**:101–115.
52 Xi H, Kurtoglu M, Liu H, Wangpaichitr M, You M, Liu X, *et al*. 2-Deoxy-D-glucose activates autophagy via endoplasmic reticulum stress rather than ATP depletion. *Cancer Chemother Pharmacol* 2011; **67**:899–910.
53 Kurtoglu M, Gao N, Shang J, Maher JC, Lehrman MA, Wangpaichitr M, *et al*. Under normoxia, 2-deoxy-D-glucose elicits cell death in select tumor types not by inhibition of glycolysis but by interfering with N-linked glycosylation. *Mol Cancer Ther* 2007; **6**:3049–3058.
54 Ho JSL, Ma W, Mao DYL, Benchimol S. p53-Dependent transcriptional repression of c-myc is required for G1 cell cycle arrest. *Mol Cell Biol* 2005; **25**:7423–7431.
55 Zhou F, Shen Q, Claret FX. Novel roles of reactive oxygen species in the pathogenesis of acute myeloid leukemia. *J Leukoc Biol* 2013; **94**:423–429.
56 Macchioni L, Davidescu M, Roberti R, Corazzi L. The energy blockers 3-bromopyruvate and lonidamine: effects on bioenergetics of brain mitochondria. *J Bioenerg Biomembr* 2014; **46**:89–394.
57 Sallmyr A, Fan J, Rassool FV. Genomic instability in myeloid malignancies: increased reactive oxygen species (ROS), DNA double strand breaks (DSBs) and error-prone repair. *Cancer Lett* 2008; **270**:1–9.